BULLETIN OF THE POLISH ACADEMY OF SCIENCES
TECHNICAL SCIENCES, Vol. 71(5), 2023, Article number: e146474
DOI: 10.24425/bpasts.2023.146474

Robust hybrid synchronization control of chaotic 3-cell CNN with uncertain parameters using smooth super twisting algorithm

Nazam SIDDIQUE[1]*, Fazal ur REHMAN[2], Uzair RAOOF[3], Shahid IQBAL[1], and Muhammad RASHAD[3]

[1] University of Gujrat, Gujrat, Pakistan
[2] Capital University of Science and Technology, Islamabad, Pakistan
[3] University of Lahore, Lahore, Pakistan

Abstract. This paper presents the control design framework for the hybrid synchronization (HS) and parameter identification of the 3-cell cellular neural network. The cellular neural network (CNN) of this kind has increasing practical importance but due to its strong chaotic behavior and the presence of uncertain parameters make it difficult to design a smooth control framework. Sliding mode control (SMC) is very helpful for this kind of environment where the systems are nonlinear and have uncertain parameters and bounded disturbances. However, conventional SMC offers a dangerous chattering phenomenon, which is not acceptable in this scenario. To get chattering-free control, smooth higher-order SMC formulated on the smooth super twisting algorithm (SSTA) is proposed in this article. The stability of the sliding surface is ensured by the Lyapunov stability theory. The convergence of the error system to zero yields hybrid synchronization and the unknown parameters are computed adaptively. Finally, the results of the proposed control technique are compared with the adaptive integral sliding mode control (AISMC). Numerical simulation results validate the performance of the proposed algorithm.

Key words: hybrid synchronization; cellular neural network; sliding mode control; smooth super twisting algorithm; Lyapunov stability theory.

1. INTRODUCTION

Chua and Yang [1] presented for the first time the terminology CNN as a cellular neural network. It is considered to be a signal-processing system comprised of a lot of processing units called cells. These cells are locally connected to perform complex tasks in a parallel processing regime. Since the cells are locally connected in CNN, this feature makes it different from other neural networks [2] which is advantageous in the sense that its implementation becomes easier in the current planar technologies [3]. Several applications of CNN are reported in the literature [4–6] after its invention, especially in image processing [7]. CNNs are non-linear complex dynamical networks and the occurrence of chaos is very obvious. From an electrical engineering perspective, CNNs are considered to be dynamical networks comprising nodes that are coupled locally to perform some information processes or to generate specific behaviors. Since CCNs exhibit chaotic behavior, in this paper HS of CNNs is investigated by employing SSTA. A smooth super twisting algorithm is a special flavor of higher order sliding mode control.

There are several techniques available in the literature which reports the synchronization of chaotic systems connected in a network [8, 9]. The techniques employed to investigate the hybrid synchronization (HS) of chaotic systems can be divided into mainly two classes. One for investigation of hybrid synchronization of chaotic systems with known parameters, and the other for unknown parameters. Most of the techniques used for investigating hybrid synchronization are based on active control [10] and direct design method [11] is investigated in such circumstances where the parameters are unknown. These techniques include sliding mode control [12], integral sliding mode control [13], pinning control [14], robust control [15], tracking control [16], backstepping control [17]. Moreover, there are many different types of synchronization like lag synchronization [18], projective synchronization [15], generalized synchronization [19], phase synchronization [20], anti-synchronization [21], complete synchronization [22], hybrid synchronization [23], etc.

The evolution of the SMC algorithm has made it the first choice for control design engineers especially when the robustness of the control technique is required. SMC can control the dynamics of nonlinear natured networks by offering robustness to external perturbation as well as matched uncertainties. In addition, it has several advantages including easy design, order reduction, and quick response. In [24], its two-step simple design procedure is described, i.e. designing a stable sliding surface and after that defining a control law to impose the sliding mode in the manifold along the system dynamics. This design procedure may not be suitable for the hybrid synchronization of CNN because of uncertain parameters and bounded disturbances due to its complex dynamics. The application of the SMC method to investigate HS of CNN requires some novel approach.

*e-mail: nazam.siddique@uog.edu.pk

Manuscript submitted 2023-01-02, revised 2023-05-04, initially accepted for publication 2023-06-25, published in October 2023.

In [25], control of nonlinear systems by employing the standard sliding mode control method is discussed. In this significant work, a couple of dissimilar sliding surfaces are designed by considering the relative degree of the system and so, SMC framework is defined to impose the sliding mode in the manifold. This control framework is complicated and the application of control laws, defined on the basis of the conventional method, leads to a dangerous phenomenon called chattering. This drawback of the conventional SMC limits its application in practical cases, particularly in CNNs. In this paper, SMC-based control algorithm is proposed. Moreover, the control laws defined are second-order type sliding modes, to impose the sliding mode to the manifold. These control laws are smooth and robust as well. To get hybrid synchronization of CNN in the existence of uncertain parameters, the design of a single sliding surface based on smooth second-order SMC gives strong motivation for this research article.

With the motivation given above, a smooth second-order SMC based on SSTA for hybrid synchronization of 3-cell CNN is considered in this article. There are two reasons for proposing SSTA. First, to achieve smooth control needed for hybrid synchronization of CNN by eliminating chattering, which is unwanted, and second, to achieve robustness contrary to the uncertainties by ensuring the correctness of sliding modes. In addition, it is considered that due to uncertainties, the parameters of the CNN are unknown. As an example, 3-cell cellular neural network is considered to check the validation of the proposed control algorithm.

2. PROBLEM FORMULATION

2.1. System description and mathematical model

A 3-cell CNN system was firstly reported in [26], which can be presented as:

$$\begin{aligned} \dot{x_1} &= -x_1 + \alpha\Psi(x_1) - \delta\Psi(x_2) - \delta\Psi(x_3), \\ \dot{x_2} &= -x_2 - \delta\Psi(x_1) + \beta\Psi(x_2) - \gamma\Psi(x_3), \\ \dot{x_3} &= -x_3 - \delta\Psi(x_1) + \gamma\Psi(x_2) + \Psi(x_3). \end{aligned} \tag{1}$$

In equation (1) x_j and $\Psi(x_j)$ are system variables and output function of j-th cell, γ, δ, α and β are the real parameters. Output $\Psi(x_j)$ is the piecewise linear function defined as: $\Psi(x_j) = 0.5|x_j+1| - 0.5|x_j-1|$, $j = 1,2,3$. In [26, 27], the chaotic behavior of equation (1) is analyzed by considering these parametric values: $\alpha = 1.24$, $\beta = 1.1$, $\gamma = 4.4$, $\delta = 3.21$, the starting conditions for the dynamic states are considered as: $x_1(0) = 0.1$, $x_2(0) = 0.1$, $x_3(0) = 0.1$. The 3-D and 2-D phase portraits of equation (1) are shown in Fig. 1a–1d.

2.2. Problem statement

The chaotic nature of the 3-cells CNN [26] is a renowned case of the CNNs. To achieve hybrid synchronization equation (1) is considered as master where as the slave systems is defined as follows:

$$\begin{aligned} \dot{y_1} &= -y_1 + \alpha\Psi(y_1) - \delta\Psi(y_2) - \delta\Psi(y_3) + \hbar_1 + \mu_1, \\ \dot{y_2} &= -y_2 - \delta\Psi(y_1) + \beta\Psi(y_2) - \gamma\Psi(y_3) + \hbar_2 + \mu_2, \\ \dot{y_3} &= -y_3 - \delta\Psi(y_1) + \gamma\Psi(y_2) + \Psi(y_3) + \hbar_3 + \mu_3, \end{aligned} \tag{2}$$

where y_1, y_2, y_3 are the system variables, $\hbar_1 + \hbar_2 + \hbar_3$ are bounded disturbances, μ_1, μ_2, μ_3 are the control inputs to be determined, and $\Psi(y_j) = 0.5|y_j+1| - 0.5|y_j-1|$, $j = 1,2,3$.

Definition 1. In the 3-cell CNN equation (1), we say that there exist HS if $\mu_i s$ are designed in such a way that the states of the slave system $y_1(t), y_2(t), y_3(t)$ satisfy the error:

$$\lim_{t\to\infty} e_i(t) = \lim_{t\to\infty} y_i(t) + qx_i(t) = 0, \quad i = 1,2,3.$$

For the anti-synchronization $q = 1$ and for the synchronization $q = -1$. The HS control becomes a problem to design appropriate controller μ_i to make $e_i(t) \to 0$ asymptotically.

3. PROPOSED CONTROL ALGORITHM AND NUMERICAL EXAMPLE

To investigate robust hybrid synchronization control of 3-cell CNN, the following two cases are considered. In case (i) smooth twisting algorithm (SSTA) is employed and in case (ii) AISMC is applied.

Case (i) Assuming γ, δ, α, β are known and defining the error as:

$$e_1 = y_1 - qx_1, \quad e_2 = y_2 - qx_2, \quad e_3 = y_3 - qx_3. \tag{3}$$

When $q = 1$, it yields synchronization and when $q = -1$, anti-synchronization is achieved. The error dynamical system is obtained as:

$$\begin{aligned} \dot{e_1} &= \dot{y_1} - q\dot{x_1} \\ &= -y_1 + \alpha\Psi(y_1) - \delta\Psi(y_2) - \delta\Psi(y_3) + \hbar_1 + \mu_1 \\ &\quad - q\{-x_1 + \alpha\Psi(x_1) - \delta\Psi(x_2) - \delta\Psi(x_3)\}, \\ \dot{e_2} &= \dot{y_2} - q\dot{x_2} \\ &= -y_2 - \delta\Psi(y_1) + \beta\Psi(y_2) - \gamma\Psi(y_3) + \hbar_2 + \mu_2 \\ &\quad - q\{-x_2 - \delta\Psi(x_1) + \beta\Psi(x_2) - \gamma\Psi(x_3)\}, \\ \dot{e_3} &= \dot{y_3} - q\dot{x_3} \\ &= -y_3 - \delta\Psi(y_1) + \gamma\Psi(y_2) + \Psi(y_3) + \hbar_3 + \mu_3 \\ &\quad - q\{-x_3 - \delta\Psi(x_1) + \gamma\Psi(x_2) + \Psi(x_3)\} \end{aligned} \tag{4}$$

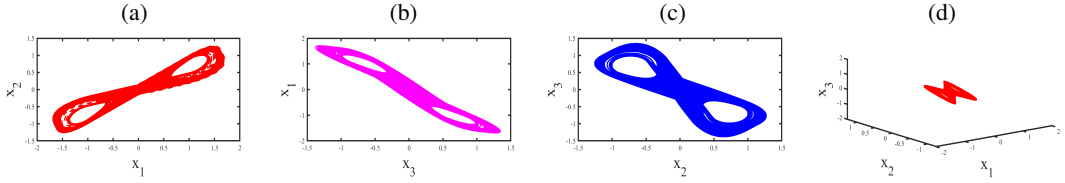

Fig. 1. Chaotic behavior of 3-cell cellular neural network on (a) x_1, x_2 space, (b) x_3, x_1 space, (c) x_2, x_3 space and (d) x_1, x_2, x_3 space

by choosing

$$\begin{aligned}\mu_1 &= y_1 - \alpha\Psi(y_1) + \delta\Psi(y_2) + \delta\Psi(y_3)\\ &\quad + q\{-x_1 + \alpha\Psi(x_1) - \delta\Psi(x_2) - \delta\Psi(x_3)\} + e_2\,,\\ \mu_2 &= y_2 + \delta\Psi(y_1) - \beta\Psi(y_2) + \gamma\Psi(y_3)\\ &\quad + q\{-x_2 - \delta\Psi(x_1) + \beta\Psi(x_2) - \gamma\Psi(x_3)\} + e_3\,,\\ \mu_3 &= y_3 + \delta\Psi(y_1) - \gamma\Psi(y_2) - \Psi(y_3)\\ &\quad + q\{-x_3 - \delta\Psi(x_1) + \gamma\Psi(x_2) + \Psi(x_3)\} + \nu,\end{aligned} \tag{5}$$

where ν is the new input then equation (4) becomes as follows:

$$\dot{e_1} = e_2 + \hbar_1\,, \quad \dot{e_2} = e_3 + \hbar_2\,, \quad \dot{e_3} = \nu + \hbar_3\,. \tag{6}$$

By choosing the Hurwitz SS for equation (6) as: $\sigma = e_1 + 2e_2 + e_3$ and its derivative is taken as:

$$\dot{\sigma} = \dot{e_1} + 2\dot{e_2} + \dot{e_3} = e_2 + 2e_3 + \nu + \hbar_1 + 2\hbar_2 + \hbar_3\,. \tag{7}$$

By selecting,

$$\nu = \nu_{eq} + \nu_s\,, \tag{8}$$

where

$$\begin{aligned}\nu_{eq} &= -e_2 - 2e_3\,,\\ \nu_s &= -\kappa_1|\sigma|^{\frac{\varphi-1}{\varphi}}\,\mathrm{sign}(\sigma) + w,\\ \dot{w} &= -\kappa_2|\sigma|^{\frac{\varphi-2}{\varphi}}\,\mathrm{sign}(\sigma), \quad \kappa_1, \kappa_2 > |\hbar_1 + \hbar_2 + \hbar_3|, \ \varphi \geq 2.\end{aligned} \tag{9}$$

The term w is intermediate control parameter and φ is the smoothing parameter. By employing equation (9) into equation (7) yields:

$$\begin{aligned}\dot{\sigma} &= -\kappa_1|\sigma|^{d}\,\mathrm{sign}(\sigma) + w,\\ \dot{w} &= -\kappa_2|\sigma|^{d-\frac{1}{\varphi}}\,\mathrm{sign}(\sigma), \quad d = \frac{\varphi-1}{\varphi}\,.\end{aligned} \tag{10}$$

Defining a new parameter as: $\zeta = \begin{bmatrix}|\sigma|^{d}\,\mathrm{sign}(\sigma)\\ w\end{bmatrix}$ and taking its derivative yields:

$$\begin{aligned}\dot{\zeta} &= \begin{bmatrix}d|\sigma|^{d-1}\dot{\sigma}\\ \dot{w}\end{bmatrix}\\ &= |\sigma|^{-\frac{1}{\varphi}}\begin{bmatrix}d - \kappa_1|\sigma|^{d}\,\mathrm{sign}(\sigma) + w\\ -\kappa_2|\sigma|^{d}\,\mathrm{sign}(\sigma)\end{bmatrix}\\ &= |\sigma|^{-\frac{1}{\varphi}}\begin{bmatrix}-d\kappa_1 & d\\ -\kappa_2 & 0\end{bmatrix}\begin{bmatrix}|\sigma|^{d}\,\mathrm{sign}(\sigma)\\ w\end{bmatrix} = |\sigma|^{-\frac{1}{\varphi}}A\zeta\,,\end{aligned} \tag{11}$$

where $A = \begin{bmatrix}-d\kappa_1 & d\\ -\kappa_2 & 0\end{bmatrix}$, i.e. $\dot{\zeta} = |\sigma|^{-\frac{1}{\varphi}}A\zeta$. The eigenvalues of A are the roots of the Hurwitz polynomial: $|\lambda I - A| = \begin{vmatrix}\lambda + d\kappa_1 & -d\\ \kappa_2 & \lambda\end{vmatrix} = \lambda^2 + \lambda(d\kappa_1) + (dk_2) = 0$, so it is strictly stable. Therefore, there is a symmetric and positive definite matrix $P \in R^{2\times 2}$ which satisfies the Lyapunov equation: $A^TP + PA = -Q$.

Theorem 1. Examine a Lyapunov function of the kind: $V = \zeta^T P\zeta$, where

$$P = \begin{bmatrix}p_1 & p_2\\ p_2 & p_3\end{bmatrix} \tag{12}$$

if equation (12) satisfies the basic Lyapunov equation: $A^TP + PA = -Q$, where $Q \in R^{2\times 2}$ is a symmetric and positive definite matrix then $\dot{V} = -|\sigma|^{-\frac{1}{\varphi}}\zeta^TQ\zeta < 0$. Consequently, equation (3) is asymptotically stable. For simulation purpose, the parametric values are set as: $\alpha = 1.24$, $\beta = 1.1$, $\gamma = 4.4$, $\delta = 3.21$.

Case (ii) Assume systems parameters are unknown and let $\hat{\gamma}$, $\hat{\delta}$, $\hat{\alpha}$, $\hat{\beta}$ be estimate of γ, δ, α, β respectively and let $\tilde{\gamma} = \gamma - \hat{\gamma}$, $\tilde{\delta} = \delta - \hat{\delta}$, $\tilde{\alpha} = \alpha - \hat{\alpha}$, $\tilde{\beta} = \beta - \hat{\beta}$ be the errors in estimating the unknown parameters. Then systems defined in equations (1) and (2) can be rewritten as:

$$\begin{aligned}\dot{x_1} &= -x_1 + \hat{\alpha}\Psi(x_1) + \tilde{\alpha}\Psi(x_1) - \hat{\delta}\Psi(x_2) - \tilde{\delta}\Psi(x_2)\\ &\quad - \hat{\delta}\Psi(x_3) - \tilde{\delta}\Psi(x_3),\\ \dot{x_2} &= -x_2 - \hat{\delta}\Psi(x_1) - \tilde{\delta}\Psi(x_1) + \hat{\beta}\Psi(x_2) + \tilde{\beta}\Psi(x_2)\\ &\quad - \hat{\gamma}\Psi(x_3) - \tilde{\gamma}\Psi(x_3),\\ \dot{x_3} &= -x_3 - \hat{\delta}\Psi(x_1) - \tilde{\delta}\Psi(x_1) + \hat{\gamma}\Psi(x_2) + \tilde{\gamma}\Psi(x_2)\\ &\quad + \Psi(x_3),\end{aligned} \tag{13}$$

$$\begin{aligned}\dot{y_1} &= -y_1 + \hat{\alpha}\Psi(y_1) + \tilde{\alpha}\Psi(y_1) - \hat{\delta}\Psi(y_2) - \tilde{\delta}\Psi(y_2)\\ &\quad - \hat{\delta}\Psi(y_3) - \tilde{\delta}\Psi(y_3) + \hbar_1 + \mu_1\,,\\ \dot{y_2} &= -y_2 - \hat{\delta}\Psi(y_1) - \tilde{\delta}\Psi(y_1) + \hat{\beta}\Psi(y_2) + \tilde{\beta}\Psi(y_2)\\ &\quad - \hat{\gamma}\Psi(y_3) - \tilde{\gamma}\Psi(y_3) + \hbar_1 + \mu_2\,,\\ \dot{y_3} &= -y_3 - \hat{\delta}\Psi(y_1) - \tilde{\delta}\Psi(y_1) + \hat{\gamma}\Psi(y_2) + \tilde{\gamma}\Psi(y_2)\\ &\quad + \Psi(y_3) + \hbar_1 + \mu_3\,.\end{aligned} \tag{14}$$

Defining the error between equations (13) and (14) as: $e_1 = y_1 - qx_1$, $e_2 = y_2 - qx_2$, $e_3 = y_3 - qx_3$. The error dynamics are obtained as:

$$\begin{aligned}\dot{e_1} &= \dot{y_1} - q\dot{x_1}\\ &= -y_1 + \hat{\alpha}\Psi(y_1) + \tilde{\alpha}\Psi(y_1) - \hat{\delta}\Psi(y_2) - \tilde{\delta}\Psi(y_2)\\ &\quad - \hat{\delta}\Psi(y_3) - \tilde{\delta}\Psi(y_3) + \hbar_1 + \mu_1 - q\{-x_1 + \hat{\alpha}\Psi(x_1)\\ &\quad + \tilde{\alpha}\Psi(x_1) - \hat{\delta}\Psi(x_2) - \tilde{\delta}\Psi(x_2) - \hat{\delta}\Psi(x_3) - \tilde{\delta}\Psi(x_3)\},\\ \dot{e_2} &= \dot{y_2} - q\dot{x_2}\\ &= -y_2 - \hat{\delta}\Psi(y_1) - \tilde{\delta}\Psi(y_1) + \hat{\beta}\Psi(y_2) + \tilde{\beta}\Psi(y_2)\\ &\quad - \hat{\gamma}\Psi(y_3) - \tilde{\gamma}\Psi(y_3) + \hbar_2 + \mu_2 - q\{-x_2 - \hat{\delta}\Psi(x_1)\\ &\quad - \tilde{\delta}\Psi(x_1) + \hat{\beta}\Psi(x_2) + \tilde{\beta}\Psi(x_2) - \hat{\gamma}\Psi(x_3) - \tilde{\gamma}\Psi(x_3)\},\\ \dot{e_3} &= \dot{y_3} - q\dot{x_3}\\ &= -y_3 - \hat{\delta}\Psi(y_1) - \tilde{\delta}\Psi(y_1) + \hat{\gamma}\Psi(y_2) + \tilde{\gamma}\Psi(y_2)\\ &\quad + \Psi(y_3) + \hbar_3 + \mu_3 - q\{-x_3 - \hat{\delta}\Psi(x_1) - \tilde{\delta}\Psi(x_1)\\ &\quad + \hat{\gamma}\Psi(x_2) + \tilde{\gamma}\Psi(x_2) + \Psi(x_3)\}.\end{aligned} \tag{15}$$

The control laws for the error dynamics defined in equation (15) can be designed in the following manner:

$$\begin{aligned}\mu_1 &= y_1 - \hat{\alpha}\Psi(y_1) + \hat{\delta}\Psi(y_2) + \hat{\delta}\Psi(y_3) \\ &\quad + q\{-x_1 + \hat{\alpha}\Psi(x_1) - \hat{\delta}\Psi(x_2) - \hat{\delta}\Psi(x_3)\} + e_2\,, \\ \mu_2 &= y_2 + \hat{\delta}\Psi(y_1) - \hat{\beta}\Psi(y_2) + \hat{\gamma}\Psi(y_3) \\ &\quad + q\{-x_2 - \hat{\delta}\Psi(x_1) + \hat{\beta}\Psi(x_2) - \hat{\gamma}\Psi(x_3)\} + e_3\,, \\ \mu_3 &= y_3 + \hat{\delta}\Psi(y_1) - \hat{\gamma}\Psi(y_2) - \Psi(y_3) \\ &\quad + q\{-x_3 - \hat{\delta}\Psi(x_1) + \hat{\gamma}\Psi(x_2) + \Psi(x_3)\} + \nu,\end{aligned} \tag{16}$$

where ν is the new input. Then the error dynamics becomes

$$\begin{aligned}\dot{e_1} &= e_2 + \tilde{\alpha}\{\Psi(y_1) - q\Psi(x_1)\} - \tilde{\delta}\{\Psi(y_2) - q\Psi(x_2)\} \\ &\quad - \tilde{\delta}\{\Psi(y_3) - q\Psi(x_3)\} + \hbar_1\,, \\ \dot{e_2} &= e_3 - \tilde{\delta}\{\Psi(y_1) - q\Psi(x_1)\} + \tilde{\beta}\{\Psi(y_2) - q\Psi(x_2)\} \\ &\quad - \tilde{\gamma}\{\Psi(y_3) - q\Psi(x_3)\} + \hbar_2\,, \\ \dot{e_3} &= v - \tilde{\delta}\{\Psi(y_1) - q\Psi(x_1)\} + \tilde{\gamma}\{\Psi(y_2) - q\Psi(x_2)\} \\ &\quad + \hbar_3\,.\end{aligned} \tag{17}$$

The Hurwitz SS for system equation (17) can be defined as: $\sigma = e_1 + 2e_2 + e_3$. Then its derivative gives:

$$\begin{aligned}\dot{\sigma} &= \dot{e_1} + 2\dot{e_2} + \dot{e_3} \\ &= e_2 + \tilde{\alpha}\{\Psi(y_1) - q\Psi(x_1)\} - \tilde{\delta}\{\Psi(y_2) - q\Psi(x_2)\} \\ &\quad - \tilde{\delta}\{\Psi(y_3) - q\Psi(x_3)\} + 2e_3 - 2\tilde{\delta}\{\Psi(y_1) - q\Psi(x_1)\} \\ &\quad + 2\tilde{\beta}\{\Psi(y_2) - q\Psi(x_2)\} - 2\tilde{\gamma}\{\Psi(y_3) - q\Psi(x_3)\} \\ &\quad + \hbar_1 + \hbar_2 - \tilde{\delta}\{\Psi(y_1) - q\Psi(x_1)\} \\ &\quad + \tilde{\gamma}\{\Psi(y_2) - q\Psi(x_2)\} + \nu + \hbar_3\,,\end{aligned} \tag{18}$$

where $\nu = \nu_0 + \nu_s$. To employ adaptive integral sliding mode control (AISMC) the following nominal system is defined.

$$\dot{e_1} = e_2\,, \quad \dot{e_2} = e_3\,, \quad \dot{e_1} = \nu_0\,. \tag{19}$$

The Hurwitz sliding surface for equation (19) is designed as $\sigma_0 = e_1 + 2e_2 + e_3$ and its first time derivative is derived as:

$$\dot{\sigma_0} = \dot{e_1} + 2\dot{e_2} + \dot{e_3}, \;\; = e_2 + 2e_3 + \nu_0\,, \tag{20}$$

By setting $\nu_0 = -e_2 - 2e_3 - \kappa * \sigma_0 * \text{sign}(\sigma_0)$, $\kappa > 0$, we have $\dot{\sigma_0} = -\kappa * \sigma_0 * \text{sign}(\sigma_0)$, which yields $\sigma_0 \to 0$ and $e_1, e_2, e_3 \to 0$. Therefore the nominal system defined in equation (19) is asymptotically stable. Now the sliding manifold for the original error dynamics defined in equation (18) can be designed as $\sigma = \sigma_0 + z$, where z is an integral term to be computed later. The time derivative of the sliding manifold designed for equation (18) is derived as:

$$\begin{aligned}\dot{\sigma} &= \dot{\sigma_0} + \dot{z} = \dot{e_1} + 2\dot{e_2} + \dot{e_3} + \dot{z} \\ &= e_2 + \tilde{\alpha}\{\Psi(y_1) - q\Psi(x_1)\} - \tilde{\delta}\{\Psi(y_2) - q\Psi(x_2)\} \\ &\quad - \tilde{\delta}\{\Psi(y_3) - q\Psi(x_3)\} + 2e_3 - 2\tilde{\delta}\{\Psi(y_1) - q\Psi(x_1)\} \\ &\quad + 2\tilde{\beta}\{\Psi(y_2) - q\Psi(x_2)\} - 2\tilde{\gamma}\{\Psi(y_3) - q\Psi(x_3)\} \\ &\quad - \tilde{\delta}\{\Psi(y_1) - q\Psi(x_1)\} + \tilde{\gamma}\{\Psi(y_2) - q\Psi(x_2)\} + \nu \\ &\quad + \hbar_1 + \hbar_2 + \hbar_3 + \dot{z}.\end{aligned} \tag{21}$$

By setting $\nu = \nu_0 + \nu_s$, where ν_s is the compensator term and ν_0 is the nominal input. The stability of the sliding manifold can be verified by the following Lyapunov stability function:

$$V = \frac{1}{2}\sigma^2 + \frac{1}{2}\left(\tilde{\gamma}^2 + \tilde{\delta}^2 + \tilde{\alpha}^2 + \tilde{\beta}^2\right). \tag{22}$$

By designing the adaptive laws $\tilde{\gamma}$, $\tilde{\delta}$, $\tilde{\alpha}$, $\tilde{\beta}$ properly and computing the compensator term ν_S, it is possible to yield $\dot{V} < 0$.

Theorem 2. For the system equation (21) it is possible to get $\dot{V} < 0$, if the adaptive laws $\tilde{\gamma}$, $\tilde{\delta}$, $\tilde{\alpha}$, integral term and the compensator term ν_s are designed as:

$$\begin{aligned}&\dot{\tilde{\gamma}} = 2l(\Psi(y_3) - q\Psi(x_3)) - l(\Psi(y_2) - q\Psi(x_2)) - \kappa_1\tilde{\gamma}, \\ &\dot{\hat{\gamma}} = -\dot{\tilde{\gamma}}, \\ &\dot{\tilde{\delta}} = l(\Psi(y_2) - q\Psi(x_2)) + l(\Psi(y_3) - q\Psi(x_3)) + l(\Psi(y_1) \\ &\qquad - q\Psi(x_1)) - \kappa_2\tilde{\delta}, \dot{\hat{\delta}} = -\dot{\tilde{\delta}} \\ &\dot{\tilde{\alpha}} = -l(\Psi(y_1) - q\Psi(x_1)) - \kappa_3\tilde{\alpha}, \dot{\hat{\alpha}} = -\dot{\tilde{\alpha}} \\ &\dot{\tilde{\beta}} = -2l(\Psi(y_2) - q\Psi(x_2)) - \kappa_4\tilde{\beta}, \dot{\hat{\beta}} = -\dot{\tilde{\beta}} \\ &\nu_s = -\kappa_5\sigma\,\text{sign}(\sigma), \;\; \nu_0 = -e_2 - 2e_3 \\ &\dot{z} = -\sigma(e_2 + 2e_3)\kappa_i > 0, i = 1, ..., 5\end{aligned} \tag{23}$$

Proof. Considering the system presented in equation (21), its first derivative is derived as:

$$\begin{aligned}\dot{V} &= \sigma\dot{\sigma} + \tilde{\delta}\dot{\tilde{\delta}} + \tilde{\gamma}\dot{\tilde{\gamma}} + \tilde{\alpha}\dot{\tilde{\alpha}} + \tilde{\beta}\dot{\tilde{\beta}} \\ &= \tilde{\alpha}\left[\sigma(\Psi(y_1) - q\Psi(x_2)) + \dot{\tilde{\alpha}}\right] + \tilde{\beta}\left[\sigma(\Psi(y_2) - q\Psi(x_2)) + \dot{\tilde{\beta}}\right] \\ &\quad + \tilde{\delta}\left[\sigma\{\tilde{\delta}(\Psi(y_2) - q\Psi(x_2)) - \tilde{\delta}(\Psi(y_3) - q\Psi(x_3)) \right. \\ &\quad \left. - 2\tilde{\delta}(\Psi(y_1) - q\Psi(x_1)) - \tilde{\delta}(\Psi(y_1) - q\Psi(x_3))\} + \dot{\tilde{\delta}}\right] \\ &\quad + \tilde{\gamma}\left[\sigma\{-2(\Psi(y_3) - q\Psi(x_3)) + (\Psi(y_2) - q\Psi(x_2)) + \dot{\tilde{\gamma}}\}\right] \\ &\quad + \left[\nu_0 + \nu_s + \hbar_1 + \hbar_2 + \hbar_3 + e_2 + 2e_3\right]\end{aligned} \tag{24}$$

by replacing the integral term, compensation terms, and adaptive laws, designed in equation (23) into equation (24) it yields:

$$\dot{V} = -\kappa_5|\sigma| - \kappa_1\tilde{\alpha}^2 - \kappa_2\tilde{\beta}^2 - \kappa_3\tilde{\delta}^2 - \kappa_4\tilde{\gamma}^2 < 0, \tag{25}$$

where κ_1, κ_2, κ_3, κ_4, $\kappa_5 > \hbar_1 + \hbar_2 + \hbar_3$. This shows that the sliding surface is asymptotically stable and the parameter estimation errors $\tilde{\alpha}$, $\tilde{\beta}$, $\tilde{\delta}$, $\tilde{\gamma} \to 0$ also the synchronization errors e_1, e_2, e_3 converges to zero. Consequently, all the states of the 3-cell CNN are in hybrid synchronization. □

4. MAIN RESULTS

Simulation results are presented by taking the following initial conditions, $x_1(0) = 12.4$, $x_2(0) = 21.7$, $x_3(0) = 10.3$, $y_1(0) = 5.3$, $y_2(0) = 23.4$, $y_3(0) = 18.7$, $\hat{\alpha}(0) = \hat{\beta}(0) = \hat{\gamma}(0) = \hat{\delta}(0) = 0$. For synchronization the initial conditions for errors are $e_1(0) = -7.1$, $e_2(0) = 1.7$, $e_3(0) = 8.4$ and for anti-synchronization the initial conditions for errors are $e_1(0) = 17.7$, $e_2(0) = 45.1$, $e_3(0) = 29$. Simulation results depicted in Figs. 2–9 are presented for Case I and simulation results depicted in Figs. 10–17 are presented for Case II. In Fig. 2 synchronization error dynamics are converging to zero which means that the states of master CNN are synchronized with the states of slave CNN. Figure 3 presents the response of the states of both the master CNN and slave CNN and it can be observed that the states are completely synchronized with each other. Figure 4 presents the control effort exerted to achieve the target. Figure 5 depicts the establishment of the sliding manifold and it can be observed very clearly that the Hurwitz SS is very smooth and there is no chattering in the steady state which validates the claim. Figure 6 displays the convergence of AS error dynamics to zero which infers that AS is achieved. Figure 7 shows the anti-synchronization of master CNN and slave CNN. Similarly, Fig. 8 represents the control effort exerted to achieve the desired goal and Fig. 9 shows the establishment of the smooth sliding surface. Figure 10 represents the convergence of synchronization error dynamics to zero for Case II where the parameters

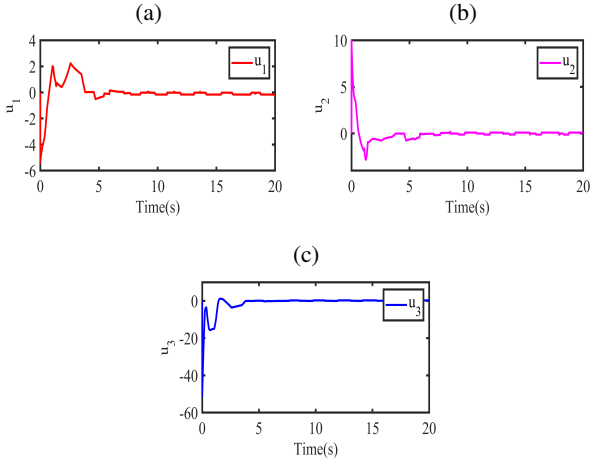

Fig. 4. Control effort exerted to achieve state synchronization between Master CNN and Slave CNN

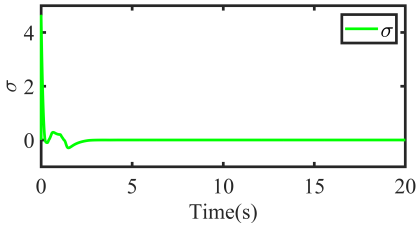

Fig. 5. Sliding Surface for synchronization in (Case I)

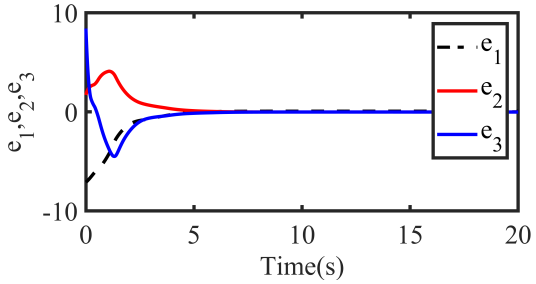

Fig. 2. Convergence of synchronization error dynamics to zero

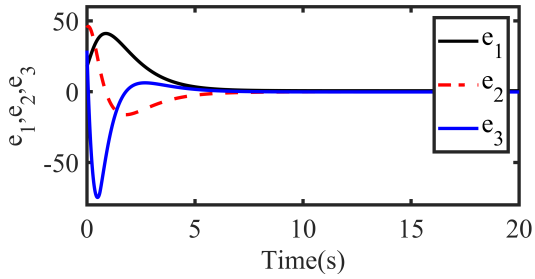

Fig. 6. Convergence of anti-synchronization error dynamic to zero (Case I)

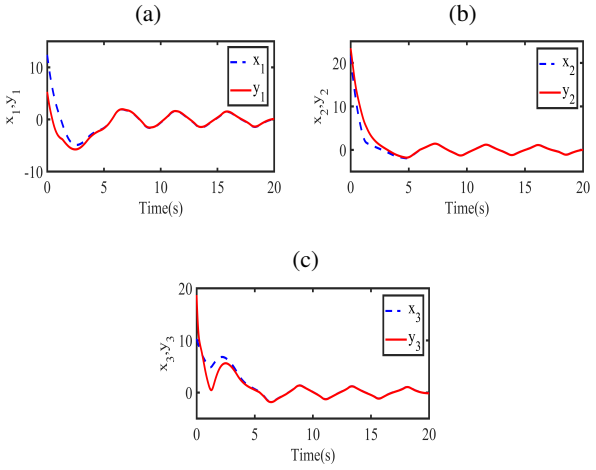

Fig. 3. States in synchronization regime of Master CNN and Slave CNN (Case I)

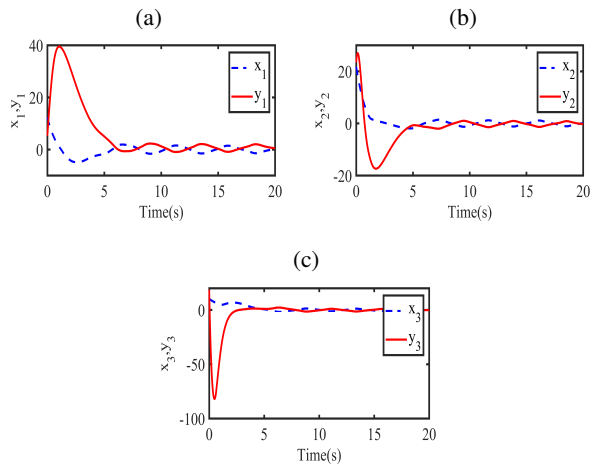

Fig. 7. States in Anti-synchronization regime of Master CNN and Slave CNN (Case I)

are assumed to be uncertain. Figure 11 presents the response of the states of both the master CNN and slave CNN and it can be observed that the states are completely synchronized with each other. Figure 12 shows the control effort exerted. Figure 13 depicts the sliding surface designed to achieve synchronization for Case II which involves chattering in the sliding phase. Figure 14 represents the convergence of anti-synchronization error dynamics to zero for Case II where the parameters are assumed to be uncertain. Figure 15 presents the response of the states of both the master CNN and slave CNN and it can be observed that the states are anti-synchronization regime. Figure 16 shows the control effort exerted. Figure 17 depicts the sliding surface designed to achieve synchronization for Case II. Figure 18 shows the convergence of α, β, γ, δ.

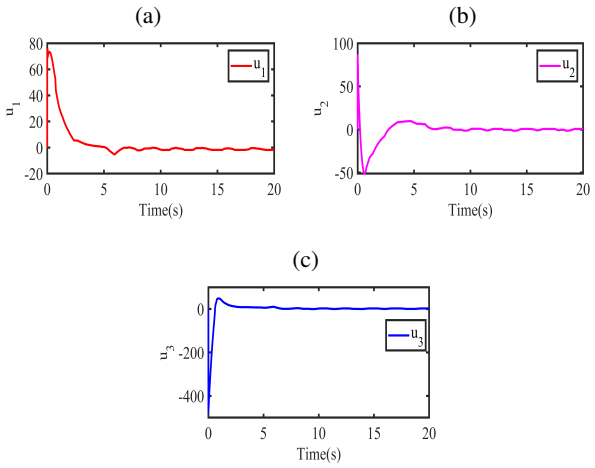

Fig. 8. Control effort exerted to achieve state Anti-synchronization between Master CNN and Slave CNN

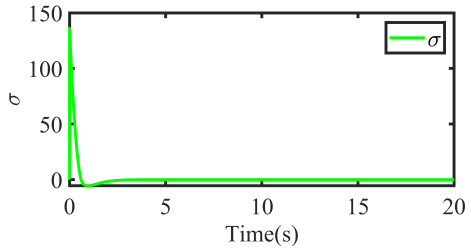

Fig. 9. Sliding surface for anti-synchronization in (Case I)

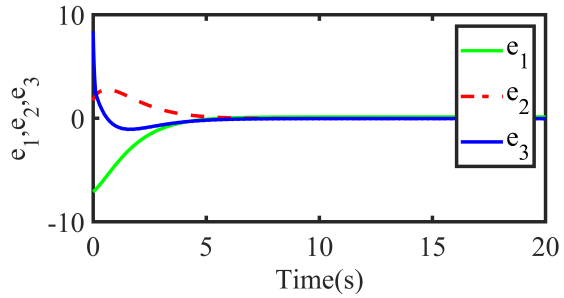

Fig. 10. Convergence of synchronization error dynamics to zero (Case II)

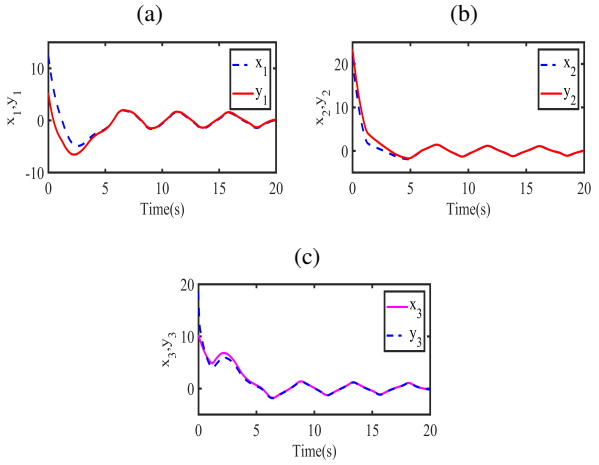

Fig. 11. States in synchronization regime of Master CNN and Slave CNN (Case II)

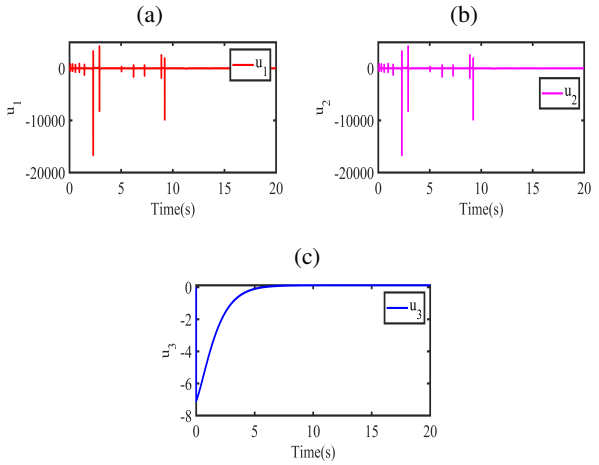

Fig. 12. Control effort exerted to achieve state synchronization between Master CNN and Slave CNN (Case II)

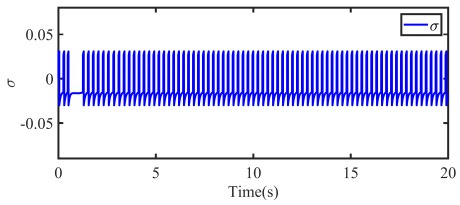

Fig. 13. Sliding surface for synchronization in (Case II)

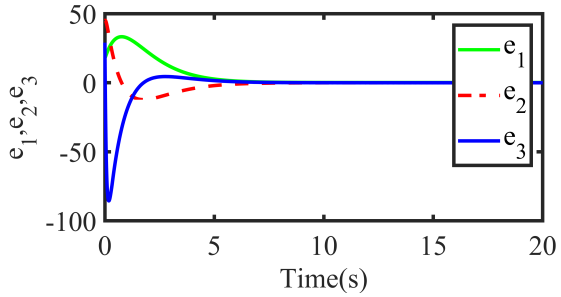

Fig. 14. Convergence of anti-synchronization error dynamics to zero (Case II)

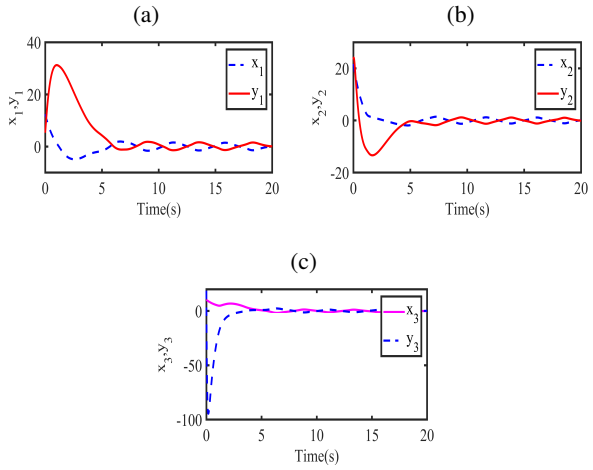

Fig. 15. States in anti-synchronization regime of Master CNN and Slave CNN (Case II)

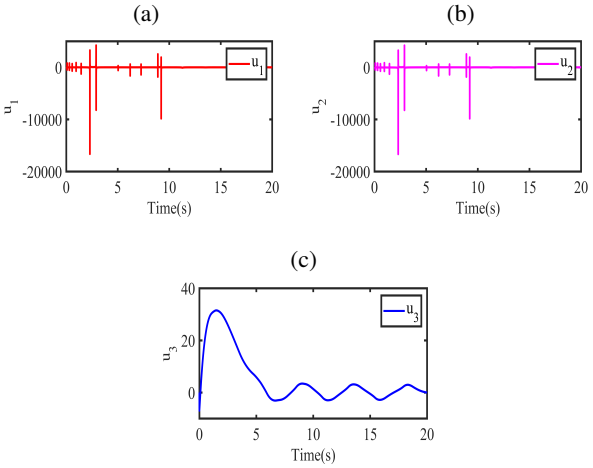

Fig. 16. Control effort exerted to achieve state anti-synchronization between Master CNN and Slave CNN

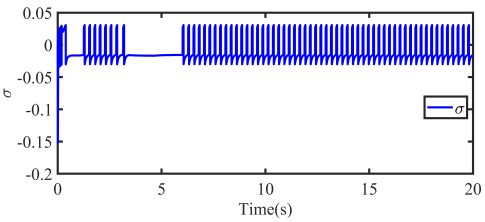

Fig. 17. Sliding surface for anti-synchronization in (Case II)

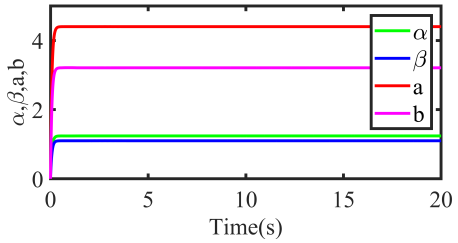

Fig. 18. Comparison of sliding manifolds designed by employing SSTA and AISMC

5. PERFORMANCE COMPARISON OF SSTA AND AISMC

Figure 19 shows the performance comparison of both the control techniques proposed in this manuscript. It can be seen that the sliding manifold designed by employing the SSTA framework presents decent steady-state characteristics. In the sliding phase, the response is very smooth and there is no unwanted phenomenon called chattering. Whereas the sliding manifold designed using AISMC comprised of chattering in the sliding phase. However, there is no chattering in the reaching phase because AISMC eliminated the reaching phase. This is a prominent feature of AISMC which makes it a suitable choice for non-linear applications where the parameters are uncertain and external disturbances are present. Both the proposed techniques performed excellently as for as the HS is concerned except for the chattering involved in the sliding phase of AISMC.

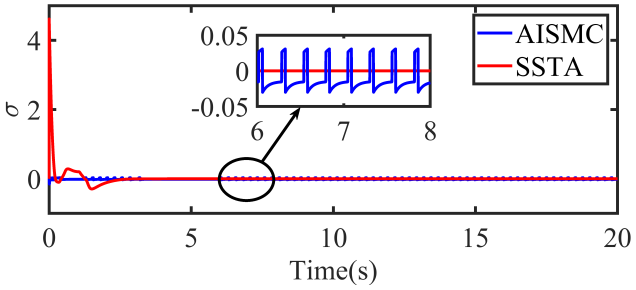

Fig. 19. Comparison of sliding manifolds designed by employing SSTA and AISMC

6. CONCLUSIONS

In this paper parameter estimation and hybrid synchronization of 3-cell cellular neural network are achieved. The methodology is based on the SSTA which is a special flavor of SOSMC. The chaotic behavior of the CNN is analyzed and the hybrid synchronization is achieved by using the Master/Slave type configuration of CNNs. A smooth sliding surface is established which ensures smooth control and robustness to external disturbances. Moreover, AISMC based control framework also presented excellent performance characteristics in the presence of bounded external disturbances and uncertain parameters. The uncertain parameters are figured out adaptively and the stability of the smooth sliding surfaces is validated by using the Lyapunov stability theorem. The effectiveness of the proposed control algorithm has been presented through extensive mathematical expressions and MATLAB simulations. The simulation results are very attractive and provide the proof of trueness of the proposed control techniques. The simulation results show the achievement of hybrid synchronization of CNNs by the proposed control laws, another key fact to remember is that the uncertain parameters converge to their real values.

REFERENCES

[1] L.O. Chua and L. Yang, "Cellular neural networks: Theory," *IEEE Trans. Circuits Syst.*, vol. 35, no. 10, pp. 1257–1272, 1988.

[2] J.M. Zurada, "Analog implementation of neural networks," *IEEE Circuits Devices*, vol. 8, no. 5, pp. 36–41, 1992.

[3] G. Liñán Cembrano, Á.B. Rodríguez Vázquez, R. Carmona Galán, F.J. Jiménez Garrido, S.C. Espejo Meana, and R. Domínguez Castro, "A 1000 fps at 128×128 vision processor with 8-bit digitized i/o," *IEEE J. Solid-State Circuits*, vol. 37, no. 7, pp. 1044–1055, 2004.

[4] P. Arena, A. Basile, M. Bucolo, and L. Fortuna, "An object oriented segmentation on analog cnn chip," *IEEE Trans. Circuits I-Fundam. Theor. Appl.*, vol. 50, no. 7, pp. 837–846, 2003.

[5] E. Tlelo-Cuautle, A.M. González-Zapata, J.D. Díaz-Muñoz, L.G. de la Fraga, and I. Cruz-Vega, "Optimization of fractional-order chaotic cellular neural networks by metaheuristics," *Eur. Phys. J.-Spec. Top.*, vol. 231, pp. 2037–2043, 2022.

[6] C. Xiu, R. Zhou, and Y. Liu, "New chaotic memristive cellular neural network and its application in secure communication system," *Chaos Solitons Fractals*, vol. 141, p. 110316, 2020.

[7] B. Belean, "Active contours driven by cellular neural networks for image segmentation in biomedical applications," *Stud. Inform. Control*, vol. 30, no. 3, pp. 109–120, 2021.

[8] X. Meng, Z. Wu, C. Gao, B. Jiang, and H.R. Karimi, "Finite-time projective synchronization control of variable-order fractional chaotic systems via sliding mode approach," *IEEE Trans. Circuits Syst. II- Express Briefs*, vol. 68, no. 7, pp. 2503–2507, 2021.

[9] F. Aliabadi, M.-H. Majidi, and S. Khorashadizadeh, "Chaos synchronization using adaptive quantum neural networks and its application in secure communication and cryptography," *Neural Comput. Appl.*, vol. 34, no. 8, pp. 6521–6533, 2022.

[10] H. Su, R. Luo, M. Huang, and J. Fu, "Practical fixed time active control scheme for synchronization of a class of chaotic neural systems with external disturbances," *Chaos Solitons Fractals*, vol. 157, p. 111917, 2022.

[11] I. Ahmad, "A lyapunov-based direct adaptive controller for the suppression and synchronization of a perturbed nuclear spin generator chaotic system," *Appl. Math. Comput.*, vol. 395, p. 125858, 2021.

[12] D. Qian, Y. Xi, and S. Tong, "Chaos synchronization of uncertain coronary artery systems through sliding mode," *Bull. Pol. Acad. Sci. Tech. Sci.*, vol. 67, no. 3, pp. 455–462, 2019.

[13] N. Siddique and F.U. Rehman, "Parameter identification and hybrid synchronization in an array of coupled chaotic systems with ring connection: An adaptive integral sliding mode approach," *Math. Probl. Eng.*, vol. 2018, p. 6581493, 2018.

[14] M. Liu, H. Jiang, C. Hu, Z. Yu, and Z. Li, "Pinning synchronization of complex delayed dynamical networks via generalized intermittent adaptive control strategy," *Int. J. Robust Nonlinear Control*, vol. 30, no. 1, pp. 421–442, 2020.

[15] G.M. Mahmoud, T. Aboelenen, T.M. Abed-Elhameed, and A.A. Farghaly, "On boundedness and projective synchronization of distributed order neural networks," *Appl. Math. Comput.*, vol. 404, p. 126198, 2021.

[16] G.M. Mahmoud, M.E. Ahmed, and T.M. Abed-Elhameed, "On fractional-order hyperchaotic complex systems and their generalized function projective combination synchronization," *Optik*, vol. 130, pp. 398–406, 2017.

[17] J. Sun, Z. Shan, P. Liu, and Y. Wang, "Backstepping synchronization control for three-dimensional chaotic oscillatory system via dna strand displacement," *IEEE Trans. Nanobiosci.*, vol. 22, no. 3, pp. 511–522, 2023.

[18] M. Yuan, X. Luo, X. Mao, Z. Han, L. Sun, and P. Zhu, "Event-triggered hybrid impulsive control on lag synchronization of delayed memristor-based bidirectional associative memory neural networks for image hiding," *Chaos Solitons Fractals*, vol. 161, p. 112311, 2022.

[19] X. Zhao, J. Liu, F. Zhang, and C. Jiang, "Complex generalized synchronization of complex-variable chaotic systems," *Eur. Phys. J.-Spec. Top.*, vol. 230, no. 7, pp. 2035–2041, 2021.

[20] X. Mao *et al.*, "Instability of optical phase synchronization between chaotic semiconductor lasers," *Opt. Lett.*, vol. 46, no. 12, pp. 2824–2827, 2021.

[21] R. Guo and Y. Qi, "Partial anti-synchronization in a class of chaotic and hyper-chaotic systems," *IEEE Access*, vol. 9, pp. 46 303–46 312, 2021.

[22] S.Z. Mirrezapour, A. Zare, and M. Hallaji, "A new fractional sliding mode controller based on nonlinear fractional-order proportional integral derivative controller structure to synchronize fractional-order chaotic systems with uncertainty and disturbances," *J. Vib. Control*, vol. 28, no. 7-8, pp. 773–785, 2022.

[23] N. Siddique and F.U. Rehman, "Hybrid synchronization and parameter estimation of a complex chaotic network of permanent magnet synchronous motors using adaptive integral sliding mode control," *Bull. Pol. Acad. Sci. Tech. Sci.*, p. e137056, 2021.

[24] V. Utkin, J. Guldner, and J. Shi, *Sliding mode control in electromechanical systems*. CRC press, 2017.

[25] R. Xu and Ü. Özgüner, "Sliding mode control of a class of underactuated systems [j]," *Automatica*, vol. 44, no. 1, pp. 233–241, 2008.

[26] P. Arena, R. Caponetto, L. Fortuna, and D. Porto, "Bifurcation and chaos in noninteger order cellular neural networks," *Int. J. Bifurcation Chaos*, vol. 8, no. 7, pp. 1527–1539, 1998.

[27] G. Manganaro, P. Arena, and L. Fortuna, *Cellular neural networks: chaos, complexity and VLSI processing*. Springer Science & Business Media, 2012, vol. 1.